

Parmalean and other siliceous nannofossils from the Oligocene of Polish Flysch Carpathians

IRENA KACZMARSKA and JAMES M. EHRMAN



Kaczmarska, I. and Ehrman, J.M. 2023. Parmalean and other siliceous nannofossils from the Oligocene of Polish Flysch Carpathians. *Acta Palaeontologica Polonica* 68 (3): 441–456.

Well-preserved fossil assemblages provide valuable insights into the evolutionary history of biota and their environments. Here, we report on Rupelian (early Oligocene) siliceous nanoeukaryotes from diatomites in the Carpathian Mountains, southeastern Poland. These sediments yielded novel forms of parmaleans and parmalean-like fossils. Their cell wall structure differs from that of described genera. Instead of the generically specific separate dorsal plate and set of girdle plates, some of our taxa contain one upended, hollow, subspherical, perforated cup. To accommodate these differences, we propose a new division Parmaphyta, a new family Parmoligocenaceae, a new genus *Parmoligocena* and a new species *Parmoligocena janusii*. Other remains are reminiscent of the extant genus *Pentalamina* and for this we propose a new genus and species, *Pentalaminamorpha radiata*. The taxonomic affinity is less certain for other nannofossils found, as they are only somewhat similar to parmaleans, and so we only tentatively associate them with this group. All these fossils occur together with a diverse assemblage of diatoms (mostly from Leptocylindrales, Rhizosoleniales, Coscinodiscales, Cymatosirales, and Hemiaulales), silicoflagellates (mostly species from the genus *Corbisema*) and archaeomonads. Together they suggest the palaeoenvironmental context for the parmaleans, a neritic marine environment, thus similar to where silicified parmaleans can be found today.

Key words: *Parmoligocena*, *Pentalaminamorpha*, diatomites, siliceous nannofossils, parmaleans, Oligocene, Polish Flysch Carpathians.

Irena Kaczmarska [jehрман@mta.ca; ORCID: <https://orcid.org/0000-0002-2527-6148>], Biology Department, Mount Allison University, Sackville, New Brunswick, E4L 1G7, Canada.

James M. Ehrman [jehрман@mta.ca; ORCID: <https://orcid.org/0000-0001-7428-2651>], Digital Microscopy Facility, Mount Allison University, Sackville, New Brunswick, E4L 1G7, Canada.

Received 21 April 2023, accepted 20 July 2023, available online 29 September 2023.

Copyright © 2023 I. Kaczmarska and J.M. Ehrman. This is an open-access article distributed under the terms of the Creative Commons Attribution License (for details please see <http://creativecommons.org/licenses/by/4.0/>), which permits unrestricted use, distribution, and reproduction in any medium, provided the original author and source are credited.

Introduction

Extant parmaleans are morphologically diverse marine photosynthetic pico- and nanoeukaryotic members of the large, well-supported supergroup TSAR (telonemids, stramenopiles, alveolates, and rhizarians). It has been postulated that TSAR may contain up to half of all eukaryote species (Burki et al. 2019; Strassert et al. 2019; Tikhonenkov et al. 2022), a great many of which remain undiscovered and/or undescribed. Under favorable growth conditions the nonflagellated parmaleans deposit siliceous components in their cell walls (Yamada et al. 2019). These organisms were discovered only relatively recently, albeit nearly two decades earlier than their nonsiliceous flagellated forms.

The siliceous, nonflagellated forms were initially considered to represent chrysophycean cysts of uncertain taxonomic affinity (Booth et al. 1980; Silver et al. 1980). A new order Parmales, two families and three genera were erected

to accommodate these taxa. Their taxonomy was based on the architecture and ornamentation of their siliceous cell wall components (Booth and Marchant 1987). They remained obscure until the extant species were grown in culture (Ichinomiya et al. 2011). The flagellated forms were discovered later than the silicified types and designated as an independent, new class of heterokonts, Bolidophyceae (Guillou et al. 1999) based on cellular and molecular data. Since then, these two life-forms have been found to be very closely related. Currently they are a rather small group containing approximately 30–40 recognised extant species of both nonsilicified, flagellated bolidomonads (1–1.7 µm in diameter) and silicified, nonflagellated parmaleans (2–5 µm in diameter; Kuwata et al. 2018; Yamada et al. 2019). Not all documented extant forms have been formally described (Konno et al. 2007; Fujita and Jordan 2017). Therefore, more parmalean diversity is anticipated given the structural variety of cell walls found in natural plankton using SEM as

well as metabarcodes recovered from environmental samples (Kuwata et al. 2018). Parma-bolidophyceans have now been documented worldwide (Kuwata et al. 2018) and are thought to contribute significantly to plankton productivity in polar and subpolar waters (Guillou 2011; Konno and Jordan 2012; Ichinomiya et al. 2019; Hoshina et al. 2021a) when and where silicate concentration in the water is relatively high (Fujita and Jordan 2017). Current understanding of their phylogenetic relationships can be found in Kuwata et al. (2018) and Yamada et al. (2019).

Siliceous components of parmalean cell walls are minute and seem to be less robustly silicified than those of most diatoms or silicoflagellates. Because of this, they are likely more susceptible to recycling during sedimentation, and dissolution during sediment diagenesis. Small cell size and apparently solitary lifestyle hampers sedimentation of parmaleans and similar microbiota throughout the water column, unless circumstances favorable for their preservation occur, e.g., perhaps within faecal pellets (Konno and Jordan 2012) or as impressions (Henderiks 2022). This may explain their absence among many otherwise relatively well-preserved microbes in siliceous seafloor and fossilised sediments. Consequently, parmaleans are only rarely documented from surface and subsurface seafloor sediments (Franklin and Marchant 1995) even in areas known to harbour them. Reports of fossilised parmaleans are equally infrequent (Stradner and Allram 1982; Abe and Jordan 2021).

Here, we document fossilised remains of silicified parmaleans, parmalean-like and similar nannofossils of less certain taxonomic affinity. These samples also contain other exceptionally well-preserved siliceous microfossils, including individual scales, diatom frustules, silicoflagellates, archaeomonads, and sponge spicules, allowing the placement of the parmaleans in their native Rupelian (early Oligocene) Central Paratethys environment, now in the Flysch Carpathians in southeastern Poland.

Nomenclatural acts.—This published work and the nomenclatural acts it contains, have been registered in PhycoBank ID: <http://phycobank.org/103784>.

Institutional abbreviations.—AGH, Academy of Mining and Metallurgy, Kraków, Poland; B, Botanischer Garten und Botanisches Museum, Berlin, Germany; DMF, Digital Microscopy Facility, Mount Allison University, Sackville, Canada; Herbarium KRAM, Herbarium Institutii Botanici, Academiae Scientorum Poloniae-Cracoviae, Kraków, Poland; KRAM, W. Szafer Institute of Botany, Polish Academy of Sciences, Kraków, Poland; NSERC, Natural Sciences and Engineering Research Council of Canada; PAS, Polish Academy of Sciences.

Other abbreviations.—CER, chloroplast endoplasmic reticulum; ICN, International Code of Nomenclature for algae, fungi, and plants; CAD, computer-aided design; LM, light microscopy; SEM, scanning electron microscopy.

Geological setting

Diatom-rich sediments and diatomites from the Skole Nappe, the external unit of the Flysch (Outer) Carpathians in southeastern Poland, occur mostly in lower Oligocene and lower Miocene strata (Kaczmarska 1982; Kotlarczyk 1982; Kotlarczyk and Kaczmarska 1987; Kotlarczyk and Leśniak 1990). The lithostratigraphy and composition of diatom flora in the Futoma Horizon in the lower Oligocene (Kotlarczyk 1982), later named Futoma Diatomite Member (Kotlarczyk et al. 2006), the lower part of the Menilite Formation of the Skole Nappe is described by Kotlarczyk and Kaczmarska (1987). Updated and comprehensive chronostratigraphy and biostratigraphy of the entire Menilite-Krosno Series is given in Kotlarczyk et al. (2006) and Kotlarczyk and Uchman (2012). There, the Futoma Member was estimated as mostly Rupelian (lower Oligocene) based on tephrostratigraphy, radioactive dating and calcareous nannofossils. Broader evolutionary history of the region may be found in Olszewska and Malata (2006) while of the entire Paratethys in Palcu and Krijgsman (2023).

The lower Oligocene diatomites and diatom-rich shales are widely distributed in southeastern Poland and were initially reported from Błażowa, Borek Nowy, Brzezówka, Dobra, Futoma, Hermanowa, Krościenko, Malawa, Rozpucie, and Średnia (Kotlarczyk 1982), altogether encompassing an area of approximately 1500 km². Currently, the lower Oligocene sedimentary and stratigraphic sequence of sites examined here is as follows: Futoma underlies Borek Nowy which in turn underlies Łubno (lithological units 5 and 6 in Kotlarczyk and Kaczmarska 1987), in the upper part of the lower Oligocene (Kotlarczyk et al. 2006; Kotlarczyk and Uchman 2012). We found parmaleans and/or parmalean-like fossils in each of these strata. The sequence covers almost all the zones NP23/24 (calcareous nannofossils) and IPM 4 (ichthyofauna) of the Rupelian stage of the Oligocene series (Kotlarczyk and Uchman 2012). Initially the Łubno diatom-rich samples examined were thought to belong to the upper Oligocene sediments (a part of the Piątkowa Horizon, Kotlarczyk and Kaczmarska 1987) but they have since been reappraised and placed in the upper part of the lower Oligocene (Kotlarczyk et al. 2006; Kotlarczyk and Uchman 2012).

Material and methods

Sampling and previous works.—Sampling was conducted at all sites and strata where the presence of diatom remains was detected using field LM or when the presence of siliceous microfossils was expected from the position in lithostratigraphic succession (Kaczmarska 1982; Kotlarczyk 1982; Kotlarczyk and Kaczmarska 1987; Kotlarczyk and Leśniak 1990). In total, 265 samples collected in the 1970s were re-examined for the presence of fossilised siliceous remains using LM water mounts. In the Futoma Diatomite Horizon (Kotlarczyk 1982), later named Futoma Diatomite

Member (Kotlarczyk et al. 2006), 74 of 123 samples were found to contain a sufficient quantity of well-preserved siliceous remains to warrant in-depth examination. In this report we focus on three samples with best preserved nannofossils collected from outcrops near the villages of Borek Nowy, Futoma, and Łubno. Their locations are shown in Kotlarczyk and Kaczmarska (1987). The most common diatom species and inferred palaeoenvironment in Borek Nowy, Futoma and Łubno samples that contain taxa reported here are listed in Kaczmarska (1982) and Kotlarczyk and Kaczmarska (1987). More recently, ecostratigraphy of the lower Oligocene of the area was refined using ichthyofauna (Kotlarczyk et al. 2006) and integrated with ichnology and calcareous nannofossil stratigraphy in Kotlarczyk and Uchman (2012). Alternative palaeoceanographic scenarios are discussed in Picha and Stranik (1999), Sachsenhofer et al. (2017), and Salata and Uchman (2019).

Laboratory processing.—Some microfossil-rich samples examined were lithified to a varying degree. Consequently, standard palaeodiatomological methods for sediment processing at the time (Kaczmarska 1973, 1976) were ineffective in disaggregating individual fossil remains. Therefore, separate protocols were applied for the lithified and softer sediments. For softer diatomites and diatom bearing shales, a combination of methods developed by Jousé (1966) and Mandra et al. (1973) were adopted. First, a few grams of each sample were crushed and left in distilled water for 2–4 weeks to allow water to permeate and soften porous sediments. Next, the sediments were treated with 3–10% HCL for 1–2 days to remove calcareous components. Samples were then washed with distilled water until the pH was near neutral, heated in a water bath and treated with the careful addition of 5% sodium carbonate and a few millilitres of 30% H₂O₂. The samples were boiled in this solution for several minutes and then cooled, decanted, and washed in distilled water several times to remove the majority of ever-present clay particles. The lithified samples resistant to disaggregation when treated as above were boiled for 10–30 minutes in 10% NaOH or KOH followed by repeated dilution and decantation. Lithified samples still containing visible aggregates were divided into two parts, with the well disintegrated fraction put aside. The aggregated fraction was boiled again in NaOH for 5 minutes, then quickly cooled and washed repeatedly in distilled water to minimise dissolution of lightly silicified microfossils in the strongly alkaline medium.

Some of the soft diatomaceous shales and diatomites contained a substantial amount of clay particles which can obscure fine structures of microfossils, particularly when examined using SEM. Clay was removed by repeated washing, with decantation after 12–24 hours to allow fossils to settle while clay particles remained suspended.

Microscopy and modelling.—Samples were processed for SEM using a Millipore vacuum filtration apparatus containing a 25 mm diameter, 1 µm pore size polytetrafluoroethylene (PTFE) membrane (Sterlitech Corp., Auburn, Washington,

USA). The material was first rinsed with 250 ml distilled water and then resuspended in 5 ml distilled water. A subsample of 0.5–1 ml of the rinsed sample was dispersed on a filter of the same type. Filters were mounted on aluminum stubs using double-sided tape, rimmed with colloidal carbon, and coated with ca. 10 nm gold in a Hummer 6.2 sputtering unit (Anatech USA, Sparks, Nevada, USA). SEM was performed at the DMF using either a JEOL JSM-5600 (JEOL USA, Inc., Peabody, Massachusetts, USA) operating at 10 kV and 8 mm working distance or a Hitachi SU3500 (Hitachi High-Technologies Canada, Inc., Etobicoke, Ontario, Canada) operating at 10 kV and 5 mm working distance.

As an aid to our interpretation of two-dimensional SEM images representing three-dimensional cells, including overall cell shape, measurement and placement of dorsal shield and ventral plates on the cells, schematic models employing those measurements and placements were prepared using OpenSCAD (<https://openscad.org>), free software for creating solid 3D CAD objects.

Cell wall structure terminology for parmaleans follows Konno and Jordan (2007).

Systematic palaeontology

Division Parmaphyta nov.

PhycoBank ID: <http://phycobank.org/103784>.

Diagnosis.—Unicellular photosynthesising heterokonts with two life-forms: biflagellated motile and nonflagellated nonmotile cells. Flagella of motile cells lack roots and transitional helices. Nonmotile cells may or may not carry multipartite siliceous walls. Parmaphytes differ from their closest relatives, Bacillariophytes, in the number of flagella (two vs one), their number of transitional plates (two vs none), role of flagella in life cycles (independent life stage vs spermatozoid present only in centric diatoms) and microtubular structure of their flagella (nine+two vs nine+none), respectively. Siliceous elements of the cell wall in Parmaphytes and diatoms also differ. Cell walls of the former are made of cups or plates on spheroidal cells. Diatom cell wall components consist of valves and telescoping girdle bands in a great variety of shapes.

Description.—Flagellated and nonflagellated unicellular photoautotrophic heterokont eukaryotes. Nonflagellated individuals of the same genetic identity in the markers thus far examined for the flagellated forms may or may not produce siliceous structures covering their cells. Known representatives with silicified cell walls have five-eight siliceous wall components currently in three distinct configurations: one dorsal hollow cup, three dorsal shield plates and one ventral plate; two dorsal shield plates, two dorsal girdle plates and one ventral plate, and finally one dorsal plate, three dorsal shield plates, three ventral girdle plates and one ventral plate. Flagellated forms are nonsilicified and have a rather simple flagellar apparatus: their flagella do not contain roots

Table 1. Cellular characteristics of parmaphytes and other heterokonts.

Group	Phaeophytes	Pelagophytes	Parmaphytes	Bacillariophytes
Cell types with flagella	meiospores, zygospores, gametes	vegetative	vegetative?	spermatozoids in centrics
Number of flagella	1 or 2	2	2	1
Position of basal bodies	above nucleus	in nuclear depression	above nucleus	above nucleus
Flagellar root(s)	present	absent	absent	absent
Transitional helix	absent	present	absent	absent
Number of transitional plate(s)	1	2	2	0
Microtubule pattern	9 + 2	9 + 2	9 + 2	9 + 0

and helices. Other cellular components of the known extant species conform to the coloured heterokont cell-type and include tubular cristate mitochondria and CER plastid system. The composition of photosynthetic pigments includes chl *a*, chl *c*₁₋₃ and fucoxanthins.

Remarks.—Parmaphyta are the sister clade to the division Bacillariophyta Karsten, 1928, in molecular phylogenies published to date. The complete life cycle of Parmaphytes is not yet known. An abbreviated comparison of cellular characteristics may be found in Table 1.

Class Bolidophyceae Guillou and Chrétiennot-Dinet in Guillou et al., 1999 secundum Ichinomiya and Lopes dos Santos in Ichinomiya et al., 2016

Remarks.—Molecular phylogenies show that the genus *Bolidomonas* Guillou and Chrétiennot-Dinet in Guillou et al., 1999, is not monophyletic. Therefore, the class Bolidophyceae ought to include the order Parmales which contains nearly genetically identical taxa in the genus *Triparma* Booth and Marchant, 1987, erected earlier (e.g., *Triparma pacifica* [Guillou and Chrétiennot-Dinet in Guillou et al., 1999] Ichinomiya and Lopes dos Santos, 2016 [= *Bolidomonas pacifica* Guillou and Chrétiennot-Dinet in Guillou et al., 1999]). Consequently, currently all bolidomonad species are included in the genus *Triparma* (Konno and Jordan 2012; Ichinomiya et al. 2016; Kuwata et al. 2018).

Order Parmales Booth and Marchant, 1987 secundum Konno and Jordan, 2007 (= Bolidomonadales Guillou and Chrétiennot-Dinet in Guillou et al., 1999).

Remarks.—Two extant families (Pentalaminaceae Marchant, 1987, and Triparmaceae Booth and Marchant, 1988) and three genera have been recognised to date in this order. Triparmaceae was erected to replace the family Octolaminaceae Booth and Marchant, 1987, which was not based on a generic name. We propose to add a new family accommodating Rupelian (early Oligocene) taxa discovered in this study and described below.

Family Parmoligocenaceae nov.

PhycoBank ID: <http://phycobank.org/103785>.

Etymology: Derived from *Parmoligocena*, the type genus for the family.

Type genus: *Parmoligocena* gen. nov.; see below.

Diagnosis.—Cell walls contain circular siliceous components including dorsal shield plates, a ventral plate, and an upended, hollow, subspherical, perforated cup.

Genus *Parmoligocena* nov.

PhycoBank ID: <http://phycobank.org/103786>.

Etymology: From Latin *parma*, a small shield; used as the base for other names referring to this group of organisms and the Oligocene strata in which the type species of *Parmoligocena janusii* was first found.

Type species: *Parmoligocena janusii* sp. nov.; by monotypy; see below.

Diagnosis.—As for the type species.

Remarks.—Our specimens do not match the diagnostic characters of any of the three currently recognised genera. The number of cell wall components makes it superficially similar to the extant genus *Pentalamina* Marchant, 1987, which has two dorsal shield plates, two girdle plates and one ventral plate. However, these wall constituents differ from our species in shape, size and relative position with respect to each other (cf. Kuwata et al. 2018). In two other genera (*Triparma* and *Tetraparma* Booth in Booth and Marchant 1987) cell walls consist of eight separate components (three dorsal shield plates, one dorsal plate, one ventral plate and three girdle plates), thus more than found in *Parmoligocena* gen. nov. Diagnoses for *Triparma* and *Tetraparma* specify that their cell walls contain three separate girdle plates (which together with the ventral plate constitute the ventral hemisphere) and a separate dorsal plate (which together with dorsal shield plates constitute the dorsal hemisphere, sensu Konno and Jordan 2007). Therefore, each of the hemispheres contains four separate components for a total of eight segments of the cell wall. In contrast, the ventral hemisphere of our new genus consists of only the ventral plate while the dorsal hemisphere is made of three dorsal shield plates and the upended, perforated cup, for a total of five siliceous cell wall components.

The relative position of the ventral plate and three dorsal shield plates are, however, similar to that in nearly all triparmacean species and in our proposed genus. The difference involves the area between the circular dorsal shield plates and the ventral plate. In other species it consists of three girdle plates (triradiate in *Tetraparma*, oblong in *Triparma*) which are also separate from the dorsal plate. In the new genus this entire area is covered by one structure (the upended perforated cup) filling up the space between the dorsal shield plates and the ventral plate (see SOM 1,

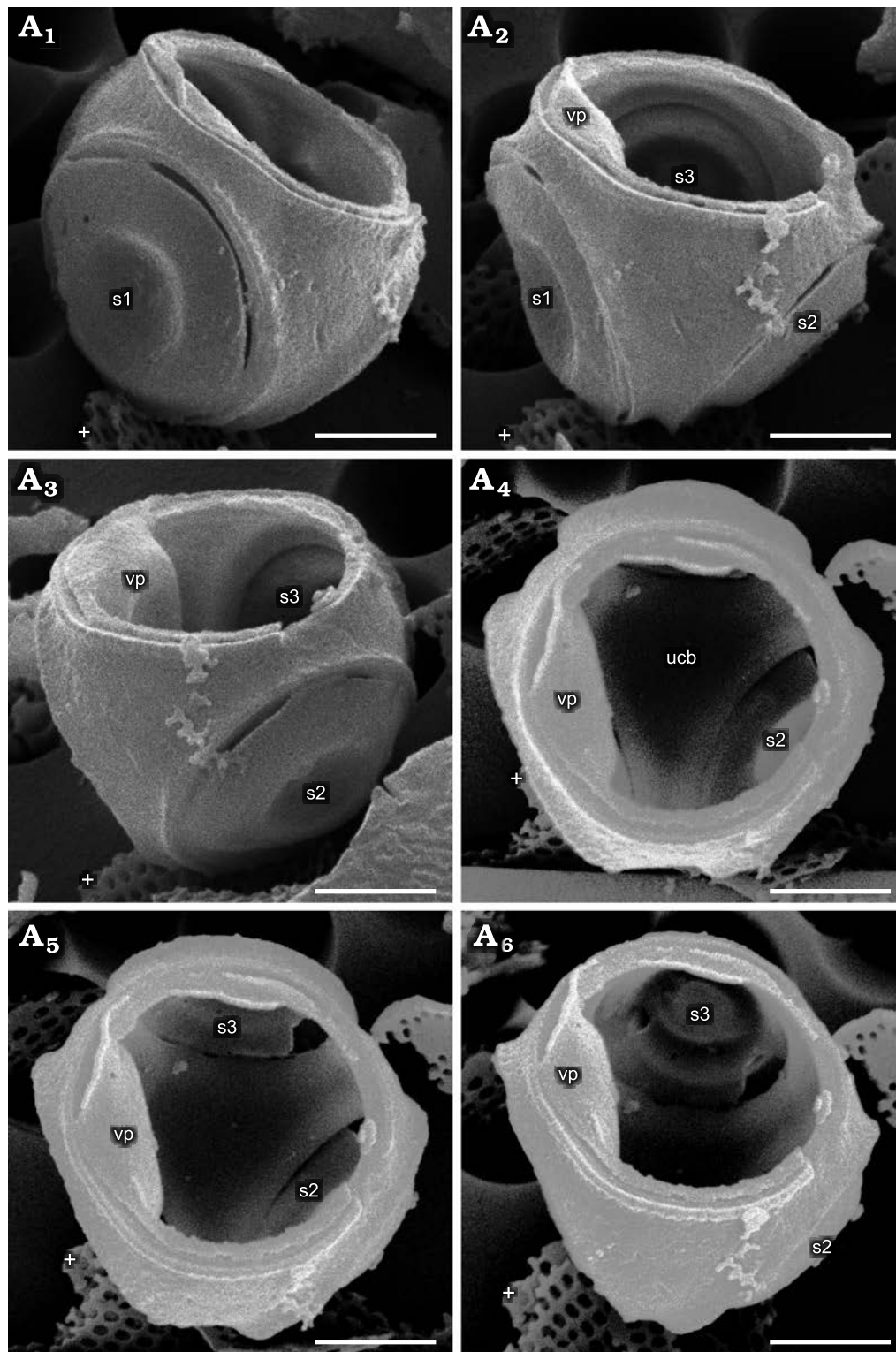


Fig. 1. Parmales from Oligocene diatomites of Poland: *Parmoligocena janusii* gen. et sp. nov. (DMF SEM stub 342-13 from Rupelian; Lubno, Poland). SEM images of a cell tilted and rotated into positions focusing on different external and internal sides of the wall. White crosses mark the same feature in each image as an aid to determining relative tilt and rotation between images. A₁, external surface of the area above and to the right of s1; A₂, external surface of the area between s1 and s2, including an internal portion above s3 in the background; vp collapsed into cell wall lumen and just its edge visible; A₃, internal view of the area between s1 (not labeled, extreme left) and s3, with vp collapsed into the cell wall lumen; A₄, internal surface of the dorsal part of ucb viewed through the ventral plate opening; vp is collapsed into the cell and can be seen at the left-hand side of the opening; A₅, a part of inner surface of the dorsal cup bottom slightly more tilted in the direction of the top of the image compared to A₄, showing lower portion of s3; A₆, interior view showing majority of the internal side of s3. Note that no seams are detectable on any of the surfaces where junctions between the dorsal plate and girdle plates appear in both *Triparma* and *Tetraparma*. Abbreviations: s1–3, arbitrarily numbered dorsal shield plates/openings; vp, ventral plate; ucb, upended dorsal cup bottom. Scale bars 1 μ m.

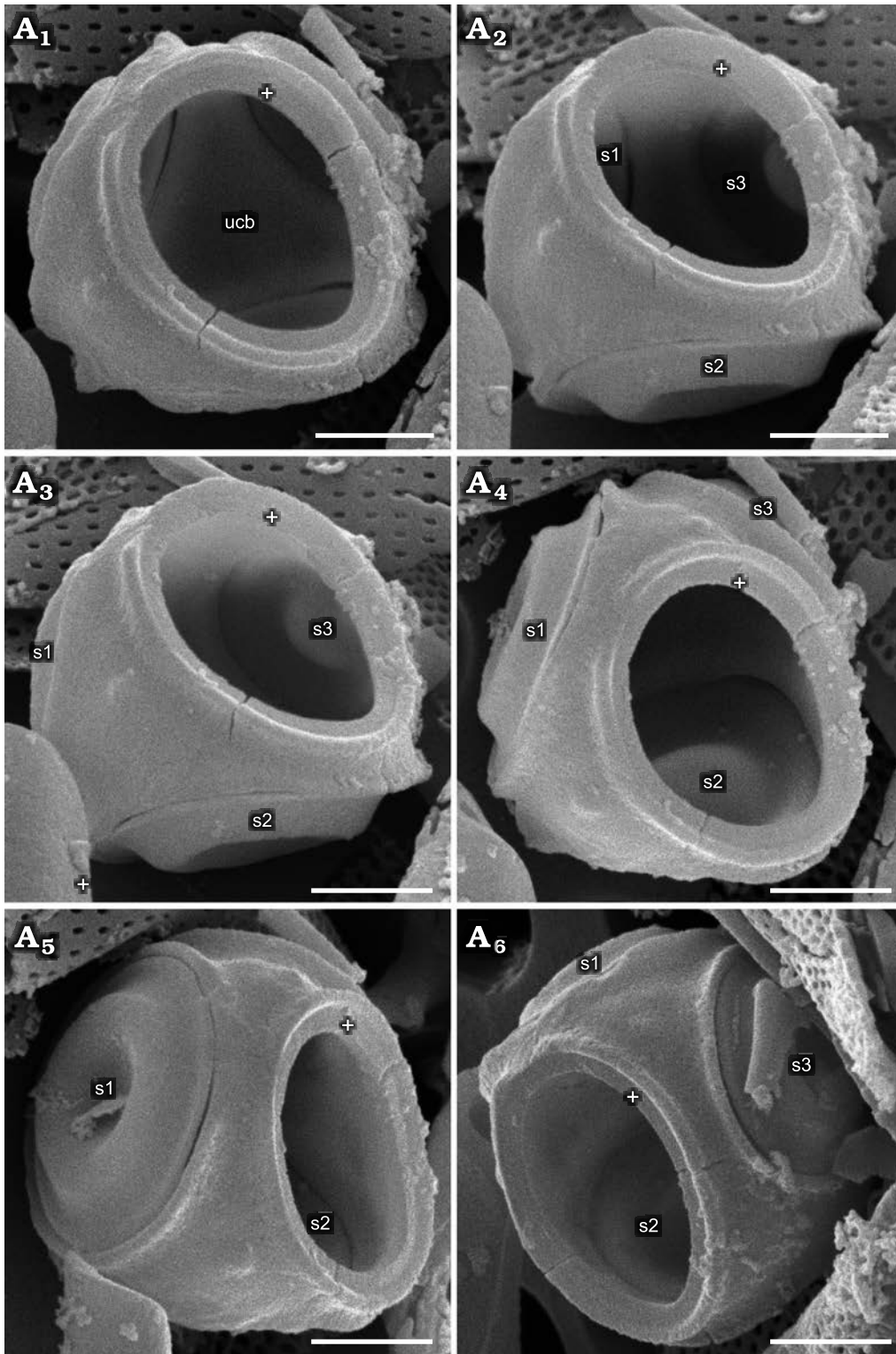


Fig. 2. Parmales from Oligocene diatomites of Poland: *Parmoligocena janusii* gen. et sp. nov. (DMF SEM stub 342-13 from Rupelian; Lubno, Poland). SEM images of a cell tilted and rotated into positions focusing on different external and internal sides of the wall. White crosses mark the same feature in each image as an aid to determining relative tilt and rotation between images. A₁, ventral plate rim and surrounding area plus internal surface of the ucb viewed through the ventral plate opening; A₂, internal surface tilted up and to the right compared to A₁, showing the upended dorsal cup wall between s1 and s3; A₃, external surface of area between s1 and s2, inside view of the area above s3; A₄, inner surface around lower part of s2 adjacent to the ucb; A₅, external surface of the area above all three dorsal shield plates and inner surface of the upper area between s2 and s3; A₆, external surface of the rim surrounding the opening for the ventral plate between s1 and s2, internal surface above the other side of s2 compared to A₅. No internal or external surfaces of the wall of the upended cup show evidence of seams. Abbreviations: s1–3, arbitrarily numbered dorsal shield plates/openings; ucb, upended dorsal cup bottom. Scale bars 1 µm.

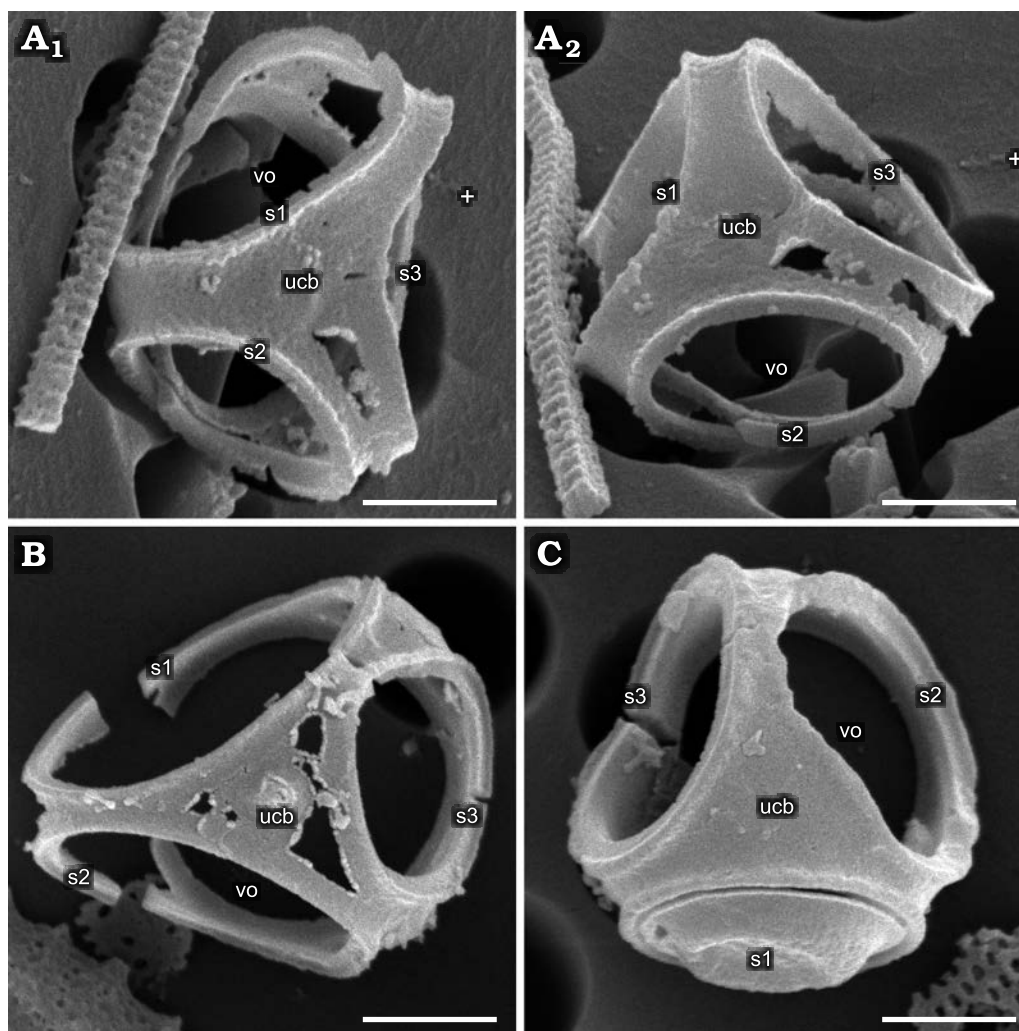


Fig. 3. Parmales from Oligocene diatomites of Poland: *Parmoligocena janusii* gen. et sp. nov. (DMF SEM stub 342-13) from Rupelian; Lubno, Poland. **A.** SEM images of one cell tilted and rotated into positions focusing on different external and internal sides of the wall. White crosses mark the same feature in each image as an aid to determining relative tilt and rotation between images; **A₁**, dorsal cup with partially eroded areas between the rims of dorsal shield plates yet no indication of seams at junctions between the sections corresponding to dorsal plate and ventral girdle plates as would be expected in *Triparma* and *Tetraparma*; **A₂**, another area of erosion between s1 and s3 openings with no breakage where a seam would be expected. **B.** A cup with greater degree of damage yet no detectable disarticulation along expected seam locations. **C.** A better-preserved cup with no sign of seams. Abbreviations: s1–3, arbitrarily numbered dorsal shield plates/openings; ucb, upended dorsal cup bottom; vo, ventral opening. Scale bars 1 μ m.

Supplementary Online Material available at http://app.pan.pl/SOM/app68-Kaczmarska_Ehrman_SOM.pdf; compare to wall elements in Kuwata et al. (2018).

Despite an extensive search, we found no evidence of separate dorsal plates or girdle plates typically seen in the two known genera from the family Triparmaceae. We examined all of the 80+ recovered identifiable fragments of such plates in our material, and through SEM stage tilt and rotation searched for evidence of a consistent breaking pattern in the cup, indicating joints between plates such as those presented in Konno and Jordan (2007), but we found none on any accessible interior and external surfaces (Figs. 1, 2). Instead, we found several dorsal upended cups maintaining their structural integrity even when the sections where seams should have been in evidence had been compromised by erosion (Fig. 3). Consequently, we conclude that our specimens have no separate dorsal plates and ventral girdle

elements. There are however species with “indistinct plates” (Fujita and Jordan 2017; Abe and Jordan 2021), and they will be discussed in the Remarks section following description of our species below.

Stratigraphic and geographic range.—As for the type species.

Parmoligocena janusii sp. nov.

Figs. 1–5, SOM 1.

Phycobank ID: <http://phycobank.org/103787>.

Etymology: Named in memory of the late Professor Janusz Kotlarczyk (1931–2017) for his insatiable and contagious enthusiasm for Polish diatomites.

Type material: Holotype, DMF SEM stub 333-10, as preparation KRAM A-25, sample Lubno 4 (Fig. 4). Isotype, DMF SEM stub 342-13 bearing approximately 24 specimens, as B 40 0046308, sample Lubno 4 (Figs. 1–3).

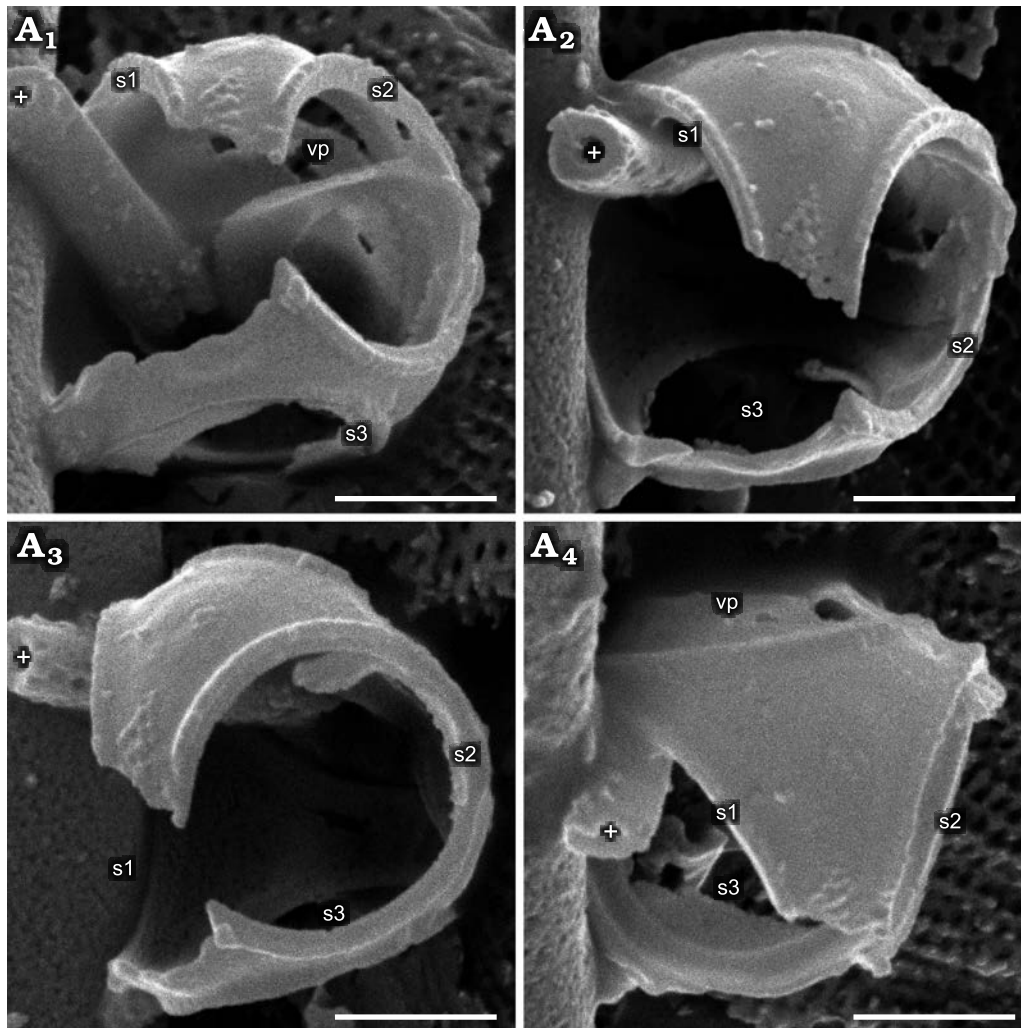


Fig. 4. Parmales from Oligocene diatomites of Poland: *Parmoligocena janusii* gen. et sp. nov. (DMF SEM stub 333-10 from Rupelian; Łubno, Poland). SEM images of a cell tilted and rotated into positions focusing on different A₁–A₄ external and internal sides of the wall. White crosses mark the same feature in each image as an aid to determining relative tilt and rotation between images. Inner surface of the partially dislodged vp can be seen in the far background in A₁ and in external profile in A₄. Abbreviations: s1–3, arbitrarily numbered dorsal shield plates/openings; vp, ventral plate. Scale bars 1 μm.

Type locality: Outcrop near the village of Łubno, southeastern Poland (shown in Kotlarczyk and Kaczmarek 1987).

Type horizon: Futoma Member, Rupelian, lower Oligocene.

Material.—Type material only.

Diagnosis.—Cell walls with five siliceous components: three circular dorsal shield plates, a hollow upended dorsal cup covering cell surface between the perforations for the dorsal shield plates and the ventral plate, and one ventral plate fitting like a lid closing the cup.

Description.—Cells subspherical (Fig. 4) with walls consisting of components organised into two unequal hemispheres. Dorsal hemisphere larger, deeper, covering most of cell surface, includes three circular shield plates (Fig. 5A, B) and one subspherical upended cup (hollow cup for convenience) with three lateral openings (Fig. 3A, B). Hollow cup includes solid triangular upended “bottom” and three long arms merging with a band surrounding circular ventral plate (Fig. 5C, D). Circular ventral plate constitutes ventral hemi-

sphere and fits like a lid on hollow cup. Dorsal shield plates and ventral plate similar with one concentric undulation separating central depression from flat marginal flange. All wall elements devoid of organised ornamentation, although some bear irregularly dispersed pores, conulae or short slits. Dorsal shield plates rest on narrow rim below inner margin of corresponding hollow in upended cup. Rims somewhat more distinctive in dorsal shield plate openings compared to ventral plate openings. Recovered remains consist of individual dorsal shield plates, ventral plates, dorsal shield plates associated with parts of dorsal cup, complete hollow cups, and nearly complete spherical walls missing only dorsal shield or ventral plates. The most often disassociated but complete components were circular dorsal shield plates and ventral plates.

Remarks.—Fifteen specimens with best preserved three-dimensional structural integrity of the siliceous shells allowed an estimate of the cell diameter that ranged between 2.80–3.56 μm (mean 3.21 μm). These specimens permit-

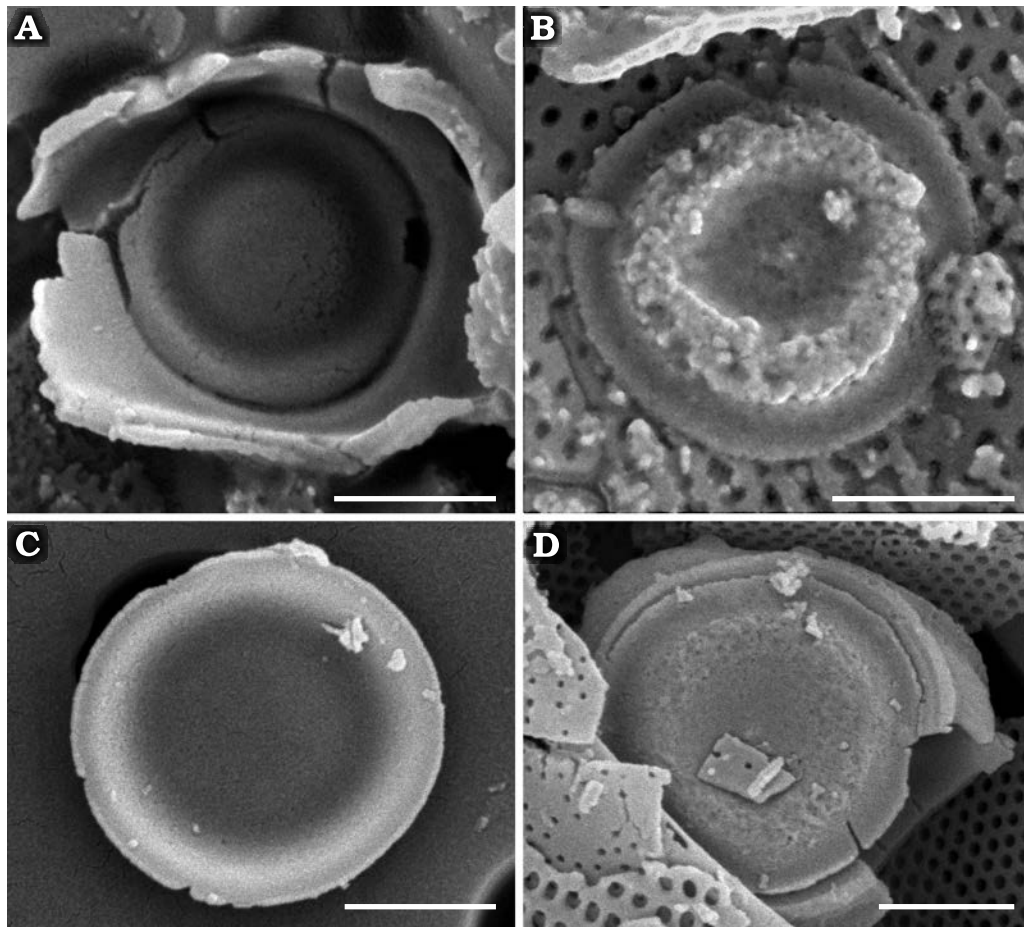


Fig. 5. *Parmoligocena janusii* gen. et sp. nov. from Rupelian (early Oligocene) diatomites of Łubno, Poland. **A, B.** DMF SEM stub 333-10. **A.** Internal surface of dorsal shield plate with notable undulations. **B.** External surface of dorsal shield plate with notable undulations. **C, D.** DMF SEM stub 342-13. **C.** Internal surface of ventral plate with less pronounced undulations. **D.** External surface of ventral plate with less pronounced undulations. Note absence of ornamentation on all plate surfaces. Scale bars 1 μm .

ted measurement of at least one dorsal shield plate and the ventral plate from the same cell (Fig. 6A). In some cells, dorsal shield plates were nearly as large as the ventral plate (difference in diameter 0.07 μm), while others were smaller by as much as 0.83 μm , with most differences falling below 0.50 μm (11 of 15 cases). In general, dorsal shield plate diameters were slightly smaller (1.51–2.39 μm , mean 2.00 μm) than ventral plates (2.15–2.77 μm , mean 2.43 μm). On intact hollow upended cups that allowed such measurements (14 of the 15 specimens above), the distance between openings for dorsal shield plates ranged between 0.22–0.56 μm (mean = 0.39 μm), while the distance between the ventral plate opening and dorsal shield plate openings ranged between 0.35–0.67 μm (mean 0.46 μm).

The overlap between the metrics for dorsal shield plates, ventral plates, and their openings on the hollow cups meant

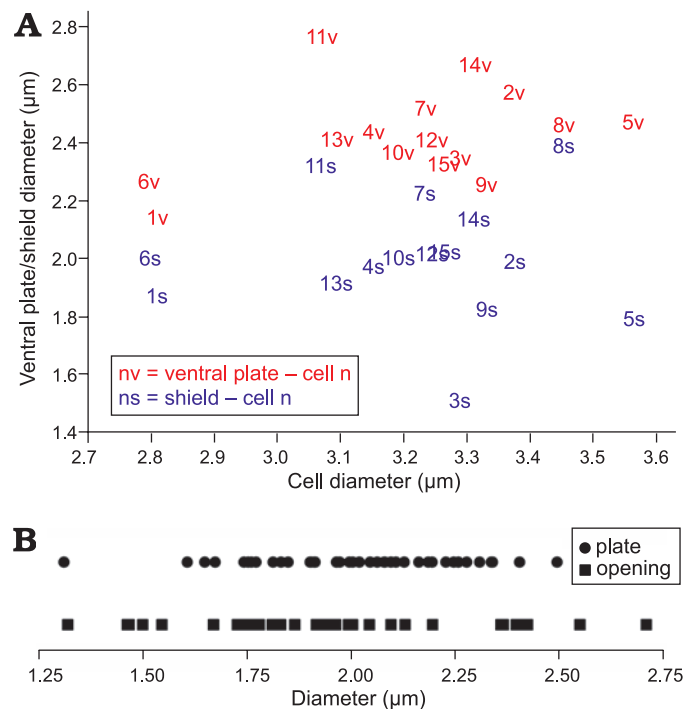


Fig. 6. *Parmoligocena janusii* gen. et sp. nov. from Oligocene diatomites of Poland. **A.** Scatterplot of dorsal shield plate and ventral plate diameters recovered from fifteen cell walls which contained at least one dorsal shield plate and a ventral plate. **B.** Diameters of individual dorsal shield plates, ventral plates and their openings recovered from fragmented dorsal hollow cups. Underlying data for Fig. 6 given in SOM 4.

Table 2. Morphometric comparison of *Parmoligocena janusii* sp. nov. with other species with apparently indistinct plate junctions. Distinguishing characters for *P. janusii* sp. nov. in bold. * metrics calculated from published images.

Feature	Taxon	<i>Tetraparma mirabilis</i>	<i>Tetraparma</i> aff. <i>mirabilis</i>	<i>Parmoligocena janusii</i> sp. nov.	“siliceous cyst”	<i>Tetraparma silverae</i>	<i>Tetraparma trullifera</i>
	Source	Abe and Jordan 2021	Abe and Jordan 2021	this study	Stradner and Allram 1982	Fujita and Jordan 2017	Fujita and Jordan 2017
Cell	Diameter (µm)	5.0–5.6	4.6–5.1	2.8–3.6	4.0–5.0	3.8–4.3	3.8–4.1
	Shape	subspherical	subspherical	subspherical	spheroid/tetrahedral	somewhat triangular	somewhat triangular
Dorsal shields	Diameter (µm)	2.4–2.7 (openings)	2.7–3.0	1.5–2.4	2.3–2.7*	2.0–2.2	3.3–3.7
	Shape	circular (openings)	circular, flat hat-shaped	circular, undulate	circular, high hat-shaped	circular, domed hat-shaped	circular, spoon-shaped
	Ornamentation	unknown	indiscernible	occasional pore	indiscernible	indiscernible	indiscernible
	Projections	unknown	absent	absent	central knobs	ribbon-like structure	flared margin
Dorsal plate	Shape	triangular?	triangular?	dorsal cup, no separate plates	triangular with humps	appeared fused to girdle	triradiate (indistinct)
	Ornamentation	indiscernible	indiscernible	occasional pore	indiscernible	indiscernible	indiscernible
	Projections	absent	absent	occasional conula	humps with knobs	absent	absent
Girdle plates	Shape	presumed fused	presumed fused	dorsal cup rim, no separate plates	unknown	triradiate (indistinct)	triradiate (indistinct)
	Ornamentation	indiscernible	indiscernible	occasional pore	indiscernible	indiscernible	indiscernible
	Projections	absent	absent	occasional conula	humps and markings	absent	absent
Ventral plate	Diameter (µm)	2.4–2.7 (openings)	2.0–3.0	2.2–2.8	2.3–2.7*	2.0–2.2	3.3–3.7
	Shape	circular (openings)	circular, flat hat-shaped	circular, undulate	circular, high hat-shaped	circular, domed hat-shaped	circular, spoon-shaped
	Ornamentation	unknown	indiscernible	occasional pore	indiscernible	indiscernible	indiscernible
	Projections	unknown	absent	absent	central knobs	ribbon-like structure	flared margin
Age		Late Cretaceous	Late Cretaceous	Rupelian (early Oligocene)	mid-late Quaternary	extant	extant

that it was challenging to differentiate between them when either separate dorsal shield plates, ventral plates or openings in cup fragments were encountered in the SEM preparations. It may be expected that, at least in part, dorsal shield plates and ventral plates may vary in size depending on the size of cells from which they came. Thus, ventral plates from smaller cells may be similar in size to dorsal shield plates from larger cells, resulting in overlap in their size distribution (Fig. 6A) and an apparent continuous size distribution of disassociated dorsal shield plates and ventral plates (Fig. 6B). Thus, we interpret this metric data as indicating that dorsal shield plates and ventral plates are not greatly different in size, with a tendency for ventral plates being somewhat larger than the dorsal shield plates.

The holotype specimen (Fig. 4) enabled the creation of an experimental schematic OpenSCAD model using its measurements for cell, dorsal shield plate and ventral plate opening radii on a presumed spherical cell. The model allows manipulation of the cell wall morphometric parameters, generating variants which then may be tilted, rotated and compared 3-dimensionally to those of the actual specimen. The OpenSCAD script for the model including adjustable parameters is given in SOM 2. The angle in which the dorsal shield plate openings extend through the hollow cup of such a hypothetical cell was then varied between 50° and 89° (with

0° placing the openings concentric at the dorsal pole of the cell). This angular range encompassed configurations where dorsal shield plate openings overlapped near the dorsal apex of the cell (50°) to where the dorsal shield plate openings impinged on the ventral plate opening (89°, see SOM 1 animation). Both extremes in angular range produced a hollow cup with overlapping openings that were not observed on any recovered specimens. More plausible dorsal shield plate opening angles varied between 60° and 70°. Measurement of distances between dorsal shield plate openings and between the ventral plate and dorsal shield plate openings in these models and comparison with actual measurements recovered indicated that dorsal shield plate openings most likely extend through the hollow cup at approximately a 64° to 65° angle. However, errors in the simulated measurements of distances between the openings compared to the actual measurements did not converge close to 0% error for both measurements, instead converging at approximately -15%, indicating that *Parmoligocena janusii* gen. et sp. nov. cells are most likely not perfectly spherical (SOM 3); hence our description of the cells as subspherical. This seems likely because if our fossil species followed the same developmental steps as extant species, plates are deposited before cup elements, thereby providing the opportunity for a spherical shape of the cell to be distorted by the stiffening of some portions before others.



Fig. 7. *Parmoligocena janusii* gen. et sp. nov. (DMF SEM stub 333-10 from Rupelian; Lubno, Poland), aggregated fragments in a presumed faecal pellet with approximate boundaries of the pellet indicated by a white frame. Digitally constructed montage of 16 individual images. Scale bar 5 μ m.

Our specimens have no immediate morphological affinity to currently recognised species (Booth and Marchant 1987; Konno et al. 2007; Fujita and Jordan 2017; Rochín-Bañaga et al. 2017; Abe and Jordan 2021; Hoshina et al. 2021a–c). If our species did have a separate dorsal plate and ventral girdle plates, it would be similar to one of the two extant genera, but to which it would belong depends on where the putative dorsal and girdle elements separate. The observed tendency for ventral plates being somewhat larger than the dorsal shield plates in our material points towards the genus *Triparma*. Smaller ventral plates compared to dorsal shield plates or equal size of these two structures is characteristic of *Tetraparma* (Konno and Jordan 2007).

Although most of the published SEM images of various species of either of the two mentioned genera show seams where plates abut or interlock, some are difficult to distinguish and may be considered fused, particularly during diagenesis and when material available for examination is scarce. According to the original authors, in three extinct and two extant taxa the nature of plate interactions remains uncertain. In Late Cretaceous *Tetraparma mirabilis* (Perch-Nielsen, 1975) Abe and Jordan, 2021, *T. aff. mirabilis*, and an unnamed “siliceous cyst” (Stradner and Allram 1982; Abe and Jordan 2021) they appear fused in some specimens while faint markings suggesting the existence of seams can be detected or are drawn on accompanying drawings (Stradner and Allram 1982). In extant *Tetraparma silverae* Fujita and Jordan, 2017, and *Tetraparma trullifera* Fujita and Jordan, 2017, the plates appear fused on some specimens, but seams can be inferred on others (Fujita and Jordan 2017). However, if their cells have the non-circular parts of the cell wall as one coherent structure, these taxa might be considered for transfer to our new genus. We also observe that in *T. mirabilis*, *T. aff. mirabilis*, *T. silverae*, and *T. trullifera*, dorsal shield plates and ventral plates are “seemingly identical in diameter and some of them also in morphology” (Fujita and Jordan 2017; Abe and Jordan 2021). This renders them atypical members of the genus *Tetraparma* (whose ventral plates are normally smaller than dorsal shield plates), but similar to some specimens of our *Parmoligocena* (Table 2). Specimens with ventral plates and dorsal shield plates of nearly equal size have been recovered in our material in addition to those of clearly different size (but not morphology), suggesting that the definite size differential between ventral plates and dorsal shield plates seen in extant genera might not yet have stabilised in all Oligocene parmaleans.

Parmoligocena janusii gen. et sp. nov. is associated with a diverse assemblage of mostly neritic diatoms from genera such as *Rhizosolenia*, *Chaetoceros* (frustules, spines and spores), *Paralia*, *Hyalodiscus*, *Actinocyclus*, and several genera from the orders Cymatosirales and Hemiaulales. A thalassiosiroid genus *Poloniasira*, fairly common in these samples, was documented in Kaczmarek and Ehrman (2008). In addition, some heavily silicified non-raphid (fragillaroid) and raphid (achnanthid, cocconeid, amphorid) taxa are also well represented. Some of them are illustrated

in Kaczmarek (1982) and Kotlarczyk and Kaczmarek (1987). Most common silicoflagellate skeletons are of several species from the genus *Corbisema*. Such fossil species composition suggests a non-oceanic environment (Kotlarczyk and Kaczmarek 1987; Kotlarczyk et al. 2006; Kotlarczyk and Uchman 2012). This is consistent with the distribution of extant silicified, non-flagellated parmaleans reported mostly from coastal waters (Konno and Jordan 2012; Kuwata and Jewson 2015). However, the polar/subpolar water temperatures that the silicified parmaleans seem to favor today (Konno and Jordan 2012; Fujita and Jordan 2017) were less likely to prevail in the Rupelian Central Paratethys. It is also evident from our material that parmalean phytoplankton have been grazed. Judging by the size of fossilised faecal pellet remains (Fig. 7) we speculate that these grazers were small filter feeders, perhaps similar to extant larvaceans (Urban et al. 1993). Konno and Jordan (2012) documented a pellet that was not attributed to any specific extant grazer but was ca. 30 µm long and 11–27 µm wide, packed with parmalean cell-wall components. This encompasses the size of the fossilised remains found here (approximately 22.5 µm long and 21.3 µm wide).

Stratigraphic and geographic range.—Rupelian, in outcrops near Łubno and Borek Nowy.

Division, class, order, and family uncertain

Genus *Pentalaminomorpha* nov.

Phycobank ID: <http://phycobank.org/103788>.

Etymology: Emphasises morphological similarity to existing genus *Pentalamina*.

Type species: *Pentalaminomorpha radiata* sp. nov.; by monotypy; see below.

Diagnosis.—As for the type species.

Pentalaminomorpha radiata sp. nov.

Fig. 8A, B.

Phycobank ID: <http://phycobank.org/103789>.

Etymology: From Latin *radius*, ray; with reference to radial ornamentation.

Holotype: DMF SEM stub 333-18, preparation KRAM A-26, sample Łubno 4 (Fig. 8A).

Type locality: Outcrop near the village of Łubno, southeastern Poland (shown in Kotlarczyk and Kaczmarek 1987).

Type horizon: Futoma Member, Rupelian, lower Oligocene.

Material.—Holotype only.

Diagnosis.—Cell walls silicified and contain elongate and circular constituents. Circular components take the form of a short, truncated cone. Elongated components are truncated isosceles triangles. Elevated central portion of the dorsal shield plates radially striated with margins showing mostly puncta and very short, parallel striae. Girdle plates perforated by disorganised pores.

Description.—Three radially ornamented structures found were circular. Most complete specimen in the form of a

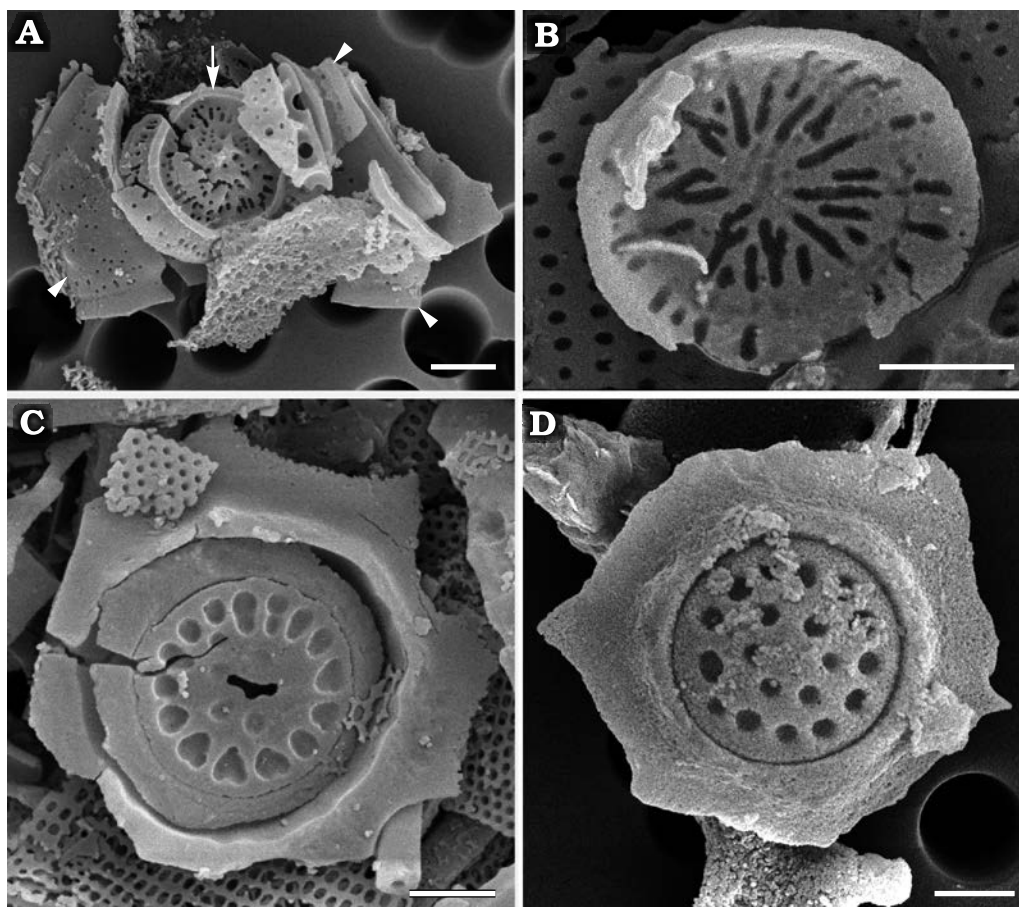


Fig. 8. Palaeomorphotaxa related or similar to parmaleans from Rupelian (lower Oligocene) diatomites of Lubno (A–C) and Futoma (D) Poland. **A.** *Pentalaminamorpha radiata* gen. et sp. nov. (DMF SEM stub 333-18), external surface of dorsal shield plate (arrow) and fragmented girdle plate (arrowheads). **B.** *Pentalaminamorpha radiata* gen. et sp. nov. (DMF SEM stub 333-10), internal view of the top of the central part of dorsal shield plate. **C.** Unnamed palaeomorphotaxon (DMF SEM stub 333-10), fragment of a cell wall containing a parmalean-like circular plate with heart-shaped depressions. **D.** Unnamed palaeomorphotaxon (DMF SEM stub 342-8), fragment of cell wall containing a plate with circular depressions. Scale bars 1 μm .

short, truncated cone with flat, ornamented top, 2.2–3.0 μm in diameter. This structure associated with triangular band with two long sides lined by marginal ridges (Fig. 8A). Ridged margins of band curve in a way suggesting formation of a hollow in which conical structures would fit. Flat tops of the conical structures ornamented by short radial, punctate striae. Subtending sides carry mixture of pores and parallel striae (Fig. 8B).

Remarks.—The conical structure is reminiscent of the dorsal shield plates in the extant parmalean genus *Pentalamina* while the rimmed band to its girdle plates. In addition, the wide side of the band also has a flange similar to what is the external surface of the curved rim along the long, left side of the triangular band. A flange in this location would be expected in a pentalaminean cell to encircle the copular ventral plate. The convex profile of the radially ornamented top and structures associated with bands that curve around in a way consistent with them fitting together is again similar to the configuration of the dorsal shield plates and ventral plates in *Pentalamina*. Altogether, these fossilised remains suggest that they might be related to parmaleans, particularly to the family Pentalaminaceae. Diagrammatic representation of

dorsal shield plates and ventral plates in extant *Pentalamina* is shown in Konno and Jordan (2007) while details of the single known species *P. corona* Marchant, 1987 in Booth and Marchant, 1987, are illustrated by Booth and Marchant (1987) and Franklin and Marchant (1995). These fossils are however notably more robust than *Parmoligocena janusii* gen. et sp. nov. or extant parmaleans in general. Cell size and complete cell walls remain unknown.

Stratigraphic and geographic range.—Type locality and horizon only.

Ornamented circular plates of unknown affinity

Fig. 8C, D.

Material.—DMF SEM stub 333-10, as preparation KRAM A-25, sample Lubno 4 and DMF SEM stub 342-8, as preparation KRAM A-27, sample Futoma 17A; from outcrops near the villages of Futoma and Lubno 4, southeastern Poland (shown in Kotlarczyk and Kaczmarska 1987); Futoma Member, Rupelian, lower Oligocene.

Description.—Flat plates inlaid in circular opening with underlying support rim (Fig. 8C, D). Plate diameter varied

between 2.4 and 3.4 μm . Largest plate ornamented by marginal ring of elongated to heart-shaped depressions and a few smaller depressions in centre. Ornamentation of two smaller plates (2.4–2.9 μm) similar, consisting of two rings of circular depressions. Plates surrounded by irregularly fractured siliceous “frames” did not allow estimation of size and shape of organism.

Remarks.—We are not aware of any extant or extinct organisms containing similar siliceous elements in their cell walls.

Discussion

The taxonomic affinity of the parmaleans was uncertain for decades and initially attributed to the class Chrysophyceae (Booth and Marchant 1987; Konno and Jordan 2007; Konno et al. 2007), albeit with reservations. However, recent molecular phylogenies have consistently indicated that they are a monophyletic sister to diatoms, and so closely related to bolidophyceans that all currently known cultured species of *Bolidomonas* were transferred to the genus *Triparma* (Kuwata et al. 2018). These authors also compared a number of cellular structures and processes in parmaleans to several groups of Stramenopiles, emphasising those that correspond to the phylogenetically high-level taxa. Such relationships already have been found in other groups of eukaryotes (Schmit and Nick 2008; De Martino et al. 2009). We expand their comparison to include derived simplification of the flagellar apparatus in two sister lineages, the diatoms and *Triparma pacifica* and compare them to more typical heterokonts (Guillou et al. 1999; Kaczmarska and Ehrman 2021; Table 1). These characters further support the notion that parmaleans and diatoms share a more recent common ancestry with each other than with other heterokonts. Nonetheless, the differences in flagellar apparatus (and genetics) between parmaleans and diatoms are profound. The diatoms show an extreme reduction in structure and a greatly restricted role of flagellated cells in the life histories of the majority of extant species (Kaczmarska and Ehrman 2021). Other cellular properties place parmaleans closer to other heterokonts than to diatoms. For example, the mitotic apparatus of *Triparma laevis* Booth in Booth and Marchant, 1987, forma *inornata* Konno, Ohira, Komuro, Harada, and Jordan, 2007, shows more ancestral features than do those in diatoms (Kuwata et al. 2018). The production of siliceous elements of the cell wall presents a more complex picture. The dorsal shield plates and ventral plates of parmaleans are deposited first and near the chloroplast (as in synurophytes and chrysophytes, Yamada et al. 2016), while the dorsal plate and ventral girdle elements are formed later and near the plasma membrane (as in diatoms, Schmid et al. 1981). The dorsal plate and ventral girdle plates fill the space between earlier deposited circular elements (Kuwata et al. 2018) at least in the experiments when cells rebuild their siliceous wall following silica starvation. This suggests the intriguing

possibility that different components of the parmalean cell wall may have a separate evolutionary history.

Furthermore, recent comparative analysis of the eight parmalean genomes and five available diatom genomes (although all are members of the same subdivision of Bacillariophytina) underscores the deep ecological, metabolic, cellular, and morphological differentiation between these two sister lineages (Ban et al. 2023). The parmaleans, presumed phago-mixotrophic nanoeukaryotes with independent silicified and nonsilicified life-stages, differ from photoautotrophic diatoms that show a greater number of gene sets involved in silica metabolism, nutrient (including iron) uptake capacity and carbon concentration mechanisms, but fewer flagellar genes. This is consistent with the observed greater degree of silicification of diatom cell-walls, species diversity, cell-size range and ecological niches colonised, when compared to parmaleans. Altogether, the differences assert that following divergence, diatoms and parmaleans have had a long and independent evolutionary history culminating in their equal but separate status as taxonomic divisions.

The exact age of the last common ancestor of parmaleans and diatoms remains a mystery. The scarce fossil record that exists for both lineages is significantly younger than the age predicted by molecular analyses (Brown and Sorhannus 2010; Strassert et al. 2021). The oldest fossilised remains generally accepted as diatoms are of the Toarcian age (Early Jurassic, ca. 190 Ma, Rothpletz 1896, 1900), while some molecular clocks predict that diatoms may be as old as ca. 540 Ma (Sims et al. 2006). The age of parmalean and diatom divergence also remains uncertain. The estimates vary from ca. 460 (Strassert et al. 2021) to 180–240 Ma (Medlin 2011). Documented fossilised remains of parmaleans are very sparse and younger than those of diatoms, dated as the Late Cretaceous (Abe and Jordan 2021). The reported but not illustrated late Eocene to mid-Miocene fossil Parmales (Thorn 2004) unfortunately cannot be substantiated. It nonetheless should be pointed out that the age of our Rupelian (early Oligocene) parmaleans (ca. 28–34 Ma) is similar to those of Thorn (2004). Lastly, the mid- to late Quaternary remains known from the Middle America Trench slope (Stradner and Allram 1982) conclude the short list of reported parmalean fossils.

Conclusions

Our results have demonstrated that Rupelian (early Oligocene) and extant silicified parmaleans are similar in size and general appearance but different in wall structure. It is also possible that the Late Cretaceous parmaleans shared more discernible cell wall characters with our Rupelian *Parmoligocena janusii* gen. et sp. nov. than with extant genera. The mechanisms differentiating cell wall hemispheres into separate dorsal shield plates and ventral plates of different sizes were either absent or not universal in Rupelian spe-

cies. We also observe that our recovered specimens demonstrate an asymmetric cell wall where one part (dorsal hollow cup) is larger and encircles a smaller ventral plate, similar to the epivalve-hypovalve configuration seen in diatoms. Such cell wall asymmetry already might have been present in the last common ancestor of parmaleans and diatoms. Based on the assemblage of diatoms, silicoflagellates, and archaeomonads occurring together with our new species, the palaeoecology of *P. janusii* gen. et sp. nov. seems similar to that of parmaleans observed today.

Furthermore, we note that although the fossil record is notoriously incomplete, samples with exceptionally well-preserved body fossils are occasionally found (e.g., Wolfe et al. 2006) and thus worth pursuing. Some of the Polish Rupelian diatomite samples belong to that rare type and yield well-preserved micro- and nannofossils from sedimentologically challenging coastal environments. Finally, we stress the significance of illustrative documentation of the remains not only because well dated fossils are unequivocal evidence of the existence of an organism at that time, but also because it provides an opportunity to examine both the nature and the rate of the evolutionary changes within the lineages.

Acknowledgements

We thank Konrad Wołowski (Department of Phycology, W. Szafer Institute of Botany, PAS, Kraków, Poland), and the administration of the W. Szafer Institute of Botany, PAS, for making this material available to us. The late Janusz Kotlarczyk (Academy of Mining and Metallurgy, Kraków, Poland) lead field expeditions. We also greatly appreciate the help provided by Michael D. Guiry (University of Galway, Ireland) in explaining nuances of the International Code of Nomenclature for algae, fungi and plants, and the late Jolanta Piątek (W. Szafer Institute of Botany, PAS, Kraków, Poland) in processing the sediment samples. This article was also greatly improved through the constructive comments provided by Wolf-Henning Kusber (Botanischer Garten und Botanisches Museum Berlin, Germany) and one anonymous reviewer. Funding for field work, sample processing and early analyses in the mid- to late 1970s was provided by the Academy of Mining and Metallurgy and the Polish Geological Institute, Warsaw, Poland. Funding for electron microscopy of siliceous microfossils was provided by an NSERC Discovery Grant and the Mount Allison University Marjorie Bell Faculty Fund (Sabbatical) awarded to IK.

References

- Abe, K. and Jordan, R.W. 2021. Re-examination of *Archaeomonas mirabilis* from the Late Cretaceous reveals its true identity as the oldest known fossil Parmales (Bolidophyceae). *Phycologia* 60: 362–367.
- Ban, H., Sato, S., Yoshikawa, S., Yamada, K., Nakamura, Y., Ichinomiya, M., Sato, N., Blanc-Mathieu, R., Endo, H., Kuwata, A., and Ogata, H. 2023. Genome analysis of Parmales, a sister group of diatoms, reveals evolutionary specialization of diatoms from phago-mixotrophs to photoautotrophs. *Communications Biology* 6: 697.
- Booth, B.C. and Marchant, H.J. 1987. Parmales, a new order of marine chrysophytes, with descriptions of three new genera and seven new species. *Journal of Phycology* 23: 245–260.
- Booth, B.C. and Marchant, H.J. 1988. Triparmaaceae, a substitute name for a family in the order Parmales (Chrysophyceae). *Journal of Phycology* 24: 124.
- Booth, B.C., Lewin, J., and Norris, R.E. 1980. Siliceous nanoplankton. I. Newly discovered cysts from the Gulf of Alaska. *Marine Biology* 58: 205–209.
- Brown, J.W. and Sorhannus, U. 2010. A molecular genetic timescale for the diversification of autotrophic Stramenopiles (Ochrophyta): substantive underestimation of putative fossil ages. *PLoS ONE* 5: e12759.
- Burki, F., Roger, A.J., Brown, M.W., and Simpson, A.G.B. 2019. The new tree of Eukaryotes. *Trends in Ecology & Evolution* 35: 43–55.
- De Martino, A., Amato, A., and Bowler, C. 2009. Mitosis in diatoms: rediscovering an old model for cell division. *Bioessays* 31: 874–884.
- Franklin, D.C. and Marchant, H.J. 1995. Parmales in sediments of Prydz Bay, East Antarctica: a new biofacies and paleoenvironmental indicator of cold water deposition? *Micropaleontology* 41: 89–94.
- Fujita, R. and Jordan, R.W. 2017. Tropical Parmales (Bolidophyceae) assemblages from the Sulu Sea and South China Sea, including the description of five new taxa. *Phycologia* 56: 499–509.
- Guillou, L. 2011. Characterization of the Parmales: much more than the resolution of a taxonomic enigma. *Journal of Phycology* 47: 2–4.
- Guillou, L., Chrétiennot-Dinet, M.-J., Medlin, L.K., Claustre, H., Loiseaux-de Goër, S., and Vaultot, D. 1999. *Bolidomonas*: a new genus with two species belonging to a new algal class, the Bolidophyceae (Heterokonta). *Journal of Phycology* 35: 368–381.
- Henderiks, J. 2022. Fossil imprints from oceans of the past. *Science* 376: 795–796.
- Hoshina, K., Narita, H., Harada, N., and Jordan, R.W. 2021a. Diversity within the *Triparma strigata*–*Triparma verrucosa* group (Bolidophyceae), including five new taxa from polar-subpolar regions. *Phycologia* 60: 215–224.
- Hoshina, K., Narita, H., Harada, N., and Jordan, R.W. 2021b. *Triparma laevis* f. *marchantii* f. nov. (Bolidophyceae) from the Southern Ocean, and comparison with other infraspecific taxa of *T. laevis*. *Phycologia* 60: 180–187.
- Hoshina, K., Uezato, Y., and Jordan, R.W. 2021c. Parmales (Bolidophyceae) assemblages in the subarctic Pacific Ocean during the mid-1960s. *Phycologia* 60: 35–47.
- Ichinomiya, M., Lopes dos Santos, A., Gourvil, P., Yoshikawa, S., Kamiya, M., Ohki, K., Audic, S., de Vargas, C., Noël, M.-H., Vaultot, D., and Kuwata, A. 2016. Diversity and oceanic distribution of the Parmales (Bolidophyceae), a picoplanktonic group closely related to diatoms. *The ISME Journal* 10: 2419–2434.
- Ichinomiya, M., Yoshikawa, S., Kamiya, M., Ohki, K., Takaichi, S., and Kuwata, A. 2011. Isolation and characterization of Parmales (Heterokonta/Heterokontophyta/Stramenopiles) from the Oyashio region, western north Pacific. *Journal of Phycology* 47: 144–151.
- Ichinomiya, M., Yamada, K., Nakagawa, Y., Nishino, Y., Kasai, H., and Kuwata, A. 2019. Parmales abundance and species composition in the waters surrounding Hokkaido, North Japan. *Polar Science* 19: 130–136.
- José, A.P. 1966. Diatomeen in Seesedimenten. *Archiv für Hydrobiologie* 4: 1–32.
- Kaczmarzka, I. 1973. Late-Glacial diatom flora at Knapówka near Włoszczowa (South Poland). *Acta Paleobotanica* 14: 179–193.
- Kaczmarzka, I. 1976. Diatom analysis of Eemian profile in freshwater deposits at Imbramowice near Wrocław. *Acta Paleobotanica* 17: 3–33.
- Kaczmarzka, I. 1982. Diatoms of the two Lower Oligocene diatomites from the Polish Carpathian Flysch. *Acta Geologica Academiae Scientiarum Hungaricae* 25: 39–47.
- Kaczmarzka, I. and Ehrman, J.M. 2008. *Poloniasira fryxelliana* Kaczmarzka, a new thalassiosiroid diatom (Bacillariophyta) from the Early Oligocene diatomites in Polish Flysch Carpathians, southeast Poland. *Nova Hedwigia, Beihefte* 133: 217–230.
- Kaczmarzka, I. and Ehrman, J.M. 2021. Enlarge or die! An auxospore perspective on diatom diversification. *Organisms Diversity & Evolution* 21: 1–23.
- Karsten, G. 1928. Abteilung Bacillariophyta (Diatomeae). *In*: A. Engler

- (ed.), *Die natürlichen Pflanzenfamilien nebst ihren Gattungen und wichtigeren Arten insbesondere den Nutzpflanzen: unter Mitwirkung zahlreicher hervorragender Fachgelehrten begründet vom A. Engler und K. Prant*, Zweite Stark, 105–303. Wilhelm Engleman, Leipzig.
- Konno, S. and Jordan, R.W. 2007. An amended terminology for the Parmales (Chrysophyceae). *Phycologia* 46: 612–616.
- Konno, S. and Jordan, R.W. 2012. Parmales. In: A. Oren and G.S. Pettis (eds.), *Encyclopedia of Life Sciences*, 1–9. John Wiley & Sons Ltd, Chichester.
- Konno, S., Ohira, R., Komuro, C., Harada, N., and Jordan, R.W. 2007. Six new taxa of subarctic Parmales (Chrysophyceae). *Journal of Nanoplankton Research* 29: 108–128.
- Kotlarczyk, J. 1982. Role of diatoms in sedimentation and biostratigraphy of the Polish Flysch Carpathians. *Acta Geologica Academiae Scientiarum Hungaricae* 25: 9–21.
- Kotlarczyk, J. and Kaczmarek, I. 1987. Two diatom horizons in the Oligocene and (?)Lower Miocene of the Polish Outer Carpathians. *Annales Societatis Geologorum Poloniae* 57: 143–188.
- Kotlarczyk, J. and Leśniak, T. 1990. *Lower Part of the Menilite Formation and Related Futoma Diatomite Member in the Skole Unit of the Polish Carpathians* [in Polish with English summary]. 74 pp. Wydawnictwo Akademii Górniczo-Hutniczej, Kraków.
- Kotlarczyk, J. and Uchman, A. 2012. Integrated ichnology and ichthyology of the Oligocene Menilite Formation, Skole and Subsilesian nappes, Polish Carpathians: a proxy to oxygenation history. *Palaeogeography, Palaeoclimatology, Palaeoecology* 331–332: 104–118.
- Kotlarczyk, J., Jerzmańska, A., Świdnicka, E., and Wiszniowska, T. 2006. A framework of ichthyofaunal ecostratigraphy of the Oligocene–Early Miocene strata of the Polish Outer Carpathian basin. *Annales Societatis Geologorum Poloniae* 76: 1–111.
- Kuwata, A. and Jewson, D.H. 2015. Ecology and evolution of marine diatoms and Parmales. In: S. Ohtsuka, T. Suzuki, T. Horiguchi, and N. Suzuki (eds.), *Marine Protists Diversity and Dynamics*, 251–275. Springer, Berlin.
- Kuwata, A., Yamada, K., Ichinomiya, M., Yoshikawa, S., Tragin, M., Vaulot, D., and Lopes dos Santos, A. 2018. Bolidophyceae, a sister picoplanktonic group of diatoms—a review. *Frontiers in Marine Science* 5: 1–17.
- Mandra, Y.T., Brigger, A.L., and Mandra, H. 1973. Chemical extraction techniques to free fossil silicoflagellates from marine sedimentary rocks. *Proceedings of the California Academy of Sciences, Series 4* 39: 273–284.
- Medlin, L.K. 2011. A review of the evolution of the diatoms from the origin of the lineage to their populations. In: J. Seckbach and P. Kociolek (eds.), *The Diatom World. Cellular Origin, Life in Extreme Habitats and Astrobiology* 19: 95–118.
- Olszewska, B. and Malata, E. 2006. Palaeoenvironmental and palaeobathymetric analysis of microfossil assemblages of the Polish Outer Carpathians [in Polish with English summary]. In: N. Oszczypko, A. Uchman, and E. Malata (eds.), *Rozwój Paleotektoniczny Basenów Karpat Zewnętrznych i Pienińskiego Pasa Skalkowego*, 61–84. Instytut Nauk Geologicznych Uniwersytetu Jagiellońskiego, Kraków.
- Palcu, D.V. and Krijgsman, W. 2023. The dire straits of Paratethys: gateways to the anoxic giant of Eurasia. *Geological Society of London Special Publications* 523: SP523–2021.
- Perch-Nielsen, K. 1975. Late Cretaceous to Pleistocene archaeomonads, ebridians, endoskeletal dinoflagellates, and other siliceous microfossils from the subantarctic southwest Pacific, DSDP, Leg 29. *Deep Sea Drilling Project* 29: 873–907.
- Picha, F.J. and Stranič, Z. 1999. Late Cretaceous to early Miocene deposits of the Carpathian foreland basin in southern Moravia. *International Journal of Earth Sciences* 88: 475–495.
- Rochín-Bañaga, H., Bollmann, J., Cortés, M.Y., and Aguirre-Bahena, F. 2017. First account of Parmales (Chrysophyceae) in sediment trap samples from the Alfonso Basin, Gulf of California, Mexico. *Journal of Coastal Research* 33: 1121–1125.
- Rothpletz, A. 1896. Über Flysch-Fucoiden und einige andere fossile Algen, sowie über liasische, Diatomeen führende Hornschwämme. *Deutsche Geologische Gesellschaft* 48: 854–914.
- Rothpletz, A. 1900. Über einen neuen jurassischen Hornschwamm und die darin eingeschlossenen Diatomeen. *Deutsche Geologische Gesellschaft* 52: 152–160.
- Sachsenhofer, R.F., Popov, S.V., Bechtel, A., Coric, S., Francu, J., Gratzner, R., Grunert, P., Kotarba, M., Mayer, J., Pupp, M., Rupprecht, B.J., and Vincent, S.J. 2017. Oligocene and Lower Miocene source rocks in the Paratethys: palaeogeographical and stratigraphic controls. In: M.D. Simmons, G.C. Tari, and A.I. Okay (eds.), *Petroleum Geology of the Black Sea. Geological Society, London, Special Publications* 464: 267–306.
- Salata, D. and Uchman, A. 2019. New interpretation of the provenance of crystalline material from Oligocene flysch deposits of the Skole Nappe, Poland: evidence from heavy minerals and clasts in the Nowy Borek section. *Geologos* 25: 163–174.
- Schmid, A.-M.M., Borowitzka, M.A., and Volcani, B.E. 1981. Morphogenesis and biochemistry of diatom cell walls. In: O. Kiermayer (ed.), *Cytomorphogenesis in Plants. Cell Biology Monographs* 8: 63–97.
- Schmit, A.C. and Nick, P. 2008. Microtubules and the evolution of mitosis. In: P. Nick (ed.), *Plant Microtubules: Development and Flexibility. Plant Cell Monographs* 11: 234–266.
- Silver, M.W., Mitchell, J.G., and Ringo, D.L. 1980. Siliceous nanoplankton. II. Newly discovered cysts and abundant choanoflagellates from the Weddell Sea, Antarctica. *Marine Biology* 58: 211–217.
- Sims, P.A., Mann, D.G., and Medlin, L.K. 2006. Evolution of the diatoms: insights from fossil, biological and molecular data. *Phycologia* 45: 361–402.
- Stradner, H. and Allram, F. 1982. Notes on an enigmatic cyst, Middle America Trench, Deep Sea Drilling Project Hole 490. *Initial Reports of the Deep Sea Drilling Project* 66: 641–642.
- Strassert, J.F.H., Irisarri, I., Williams, T.A., and Burki, F. 2021. A molecular timescale for eukaryote evolution with implications for the origin of red algal-derived plastids. *Nature Communications* 12: 1879.
- Strassert, J.F.H., Jamy, M., Mylnikov, A.P., Tikhonenkov, D.V., and Burki, F. 2019. New phylogenetic analysis of the enigmatic phylum Telonemia further resolves the eukaryote tree of life. *Molecular Biology and Evolution* 36: 757–765.
- Thorn, V.C. 2004. Data report: Phytoliths in drill core sediments from Sites 1165 and 1166, Leg 188, Prydz Bay, East Antarctica. In: A.K. Cooper, P.E. O'Brien, and C. Richter (eds.), *Proceedings of the Ocean Drilling Program, Scientific Results* 188, 1–12. Texas A&M University, College Station.
- Tikhonenkov, D.V., Jamy, M., Borodina, A.S., Belyaev, A.O., Zagumyonny, D.G., Prokina, K.I., Mylnikov, A.P., Burki, F., and Karpov, S.A. 2022. On the origin of TSAR: morphology, diversity and phylogeny of Telonemia. *Open Biology* 12: 210325.
- Urban, J.L., McKenzie, C.H., and Deibel, D. 1993. Nanoplankton found in fecal pellets of macrozooplankton in coastal Newfoundland waters. *Botanica Marina* 36: 267–281.
- Wolfe, A.P., Edlund, M.B., Sweet, A.R., and Creighton, S.D. 2006. A first account of organelle preservation in Eocene non-marine diatoms: observations and paleobiological implications *Palaaios* 21: 289–304.
- Yamada, K., Katsura, H., Noël, M.-H., Ichinomiya, M., Kuwata, A., Sato, S., and Yoshikawa, S. 2019. Ontogenetic analysis of siliceous cell wall formation in *Triparma laevis* f. *inornata* (Parmales, Stramenopiles). *Journal of Phycology* 55: 196–203.
- Yamada, K., Yoshikawa, S., Ohki, K., Ichinomiya, M., Kuwata, A., Motomura, T., and Nagasato, C. 2016. Ultrastructural analysis of siliceous cell wall regeneration in the stramenopile *Triparma laevis* (Parmales, Bolidophyceae). *Phycologia* 55: 602–609.